Arch. Mech., **52**, 4–5, pp. 629–644, Warszawa 2000

On the limit analysis of defective pipelines under complex loadings

Dedicated to Professor Zenon Mróz
on the occasion of his 70th birthday

Y. LIU, B. XU and B. YANG

Department of Engineering Mechanics, Tsinghua University,
Beijing 100084, P.R. China

THE INTEGRITY ASSESSMENT of defective pipelines represents a practically important task of structural analysis and design in various technological areas, such as oil and gas industry, power plant engineering and chemical factories. It is very essential to evaluate the load-carrying capacities of defective pipelines in order to judge safely their working life. In this paper, an iterative algorithm is presented for the kinematic limit analysis of 3-D rigid-perfectly plastic bodies. A numerical path scheme for radial loading is adopted to deal with complex multi-loading systems. The numerical procedure has been applied to carry out the plastic collapse analysis of pipelines with part-through slots under internal pressure, bending moment and axial force. The effects of various shapes and sizes of part-through slots on the collapse loads of pipelines are systematically investigated and evaluated. Some typical failure modes corresponding to different configurations of slots and loading forms are studied.

Key Words: limit analysis, loading path, mathematical programming, pipeline, part-through slot

1. Introduction

PLASTIC LIMIT ANALYSIS plays a significant role in the integrity assessment of defective pipelines. The plastic limit load, which determines the carrying capacity of structures, is an important parameter in performing the two-criteria assessment of structural integrity [1]. In the ASME stress classification framework for pressure vessel design, stresses are classified as the primary, secondary and peak stresses, different admissible values are provided for different stress modes, and the admissible value of primary stress corresponds to the stress state under the limit load. Therefore, the knowledge of limit loads of mechanical components and structures is useful to the designer to address the modes of failure associated with load-controlled effects.

However, the determination of limit loads is by no means an easy task, es-

pecially for complex configurations and loading systems. Therefore, the problem how to determine the limit load efficiently and accurately has attracted the attention of many researchers. With the progress in the finite element technique and mathematical optimization theory, the simplified analysis methods for the computation of plastic limit load have been developed rapidly, such as the GLOSS r-node method of SESHADRI and FERNANDO [2], the elastic compensation method of MACKENZIE and BOYLE [3], the thermoparameter method [4] and mathematical programming methods [5 – 10], etc. The mathematical programming methods can determine the load-carrying capacity of a rigid-perfectly plastic body, which do not concern the loading process and can overcome the difficulties by step-by-step elastic-plastic analysis. The lower and upper bounds of limit load for a perfectly rigid-plastic body can be approached by mathematical programming processes based on the static and kinematic theorems of limit analysis. In comparison with the lower bound analysis, there are more difficulties in the upper bound limit analysis. Because of the nonlinearity and nonsmoothness of the objective function, many existing solution methods for mathematical programming problems cannot be used directly for an upper bound analysis. Although the numerical difficulties have been overcome by some investigators, such as HUH [7], LIU [8], CHEN [9] and ZHANG [10], these methods were mainly presented for single loading or simple 2-D structures. The numerical algorithms for the limit analysis of 3-D structures under multi-loading systems need further study and development.

Pipelines are widely used in various fields such as the petrochemical industry, energy and electric power engineering, etc. During their operation, many local defects such as part-through slots shown in Fig. 4 can be produced by corrosion, mechanical damage or abrasive surface cracks. These defects may jeopardize the integrity (i.e. reduce the load-carrying capacity) of pipelines and sometimes even lead to severe industrial accidents. The integrity assessment of defective pipelines is a very important research subject, with a significant and extensive application background in the pipeline industry. Part-through slots, which can be commonly found on the surfaces of pipelines, are classsified as a type of 3-D volumetric defects. They can result not only in stress concentration, but also in the cracks under fatigue loads. Because of the lack of systematic theoretical analyses as well as satisfactory experimental results, the effects of part-through slots on the strength of pipelines are at present still unclear. The current testing codes and standards for the pipelines in service provide severe limitations to the allowable values of part-through slots. Unnecessary welding treatments of part-through slots required by the codes, are not only resource-consuming processes but also can produce more severe welding defects. Therefore, some serious and systematic attempts should be made to investigate the effects of part-through slots on the load-carrying capacities of pipelines. These attempts are expected

to provide some more scientific and reasonable approaches for defect assessment and treatment, which will significantly reduce the resource consumption in defect treatment but still guarantee the operation safety of the pipelines. Unfortunately, only few research efforts on the plastic collapse analysis of pipelines with various part-through slots have been made up to now.

In the present study, a kinematic approach to the limit analysis of 3-D structures is proposed by means of a direct iterative algorithm. A radial loading path scheme is presented to deal with multi-loading systems. Furthermore, by using the present algorithm, the plastic collapse analysis of defective pipelines is performed under the combinations of two loads of three possible types: internal pressure, bending moment and axial force. The defects considered here include part-through spherical, ellipsoidal and rectangular slots. The limit loads of pipelines are computed for a comprehensive range of geometric parameters.The effects of various shapes and sizes of typical part-through slots on the collapse loads of pipelines are investigated. Some typical failure modes corresponding to different dimensions of slots and loading conditions are analyzed.

2. The radial loading path scheme

To present a loading path scheme used in the numerical limit analysis, we take here as an example a biaxial loading system composed of $\overline{P}_1$ and $\overline{P}_2$. The loading scheme used here is applicable to a more general muti-loading system. As shown in Fig. 1, let the slope of the ray be $\tan\theta = \dfrac{\overline{P}_2}{\overline{P}_1}$, i.e. $\overline{P}_2 = \overline{P}_1 \tan\theta \left(0 \leq \theta \leq \dfrac{\pi}{2}\right)$, where the variation of $\tan\theta$ corresponds to different loading paths which are dependent on the multi-loading systems. At each computation of the limit load multiplier performed by an iterative algorithm (see the next section for the details), take some slope of the loading path $\tan\theta$, namely, fix the relative magnitudes of different loads $\overline{P}_1$ and $\overline{P}_2$. When θ changes from 0 to 90 degrees, the limit state at each last iteration composes the complete limit load interaction curve as shown in Fig. 1. In particular, when θ is equal to 0 or 90 degrees, the iteration solution is the limit load solution corresponding to $\overline{P}_1$ or $\overline{P}_2$. For a rigid-perfectly plastic material, this scheme of loading path can be extended to the limit analysis under the combined action of three loading systems.

For generalized loadings $\langle \overline{P}_1, \overline{P}_2 \rangle$, we have:

$$\langle \overline{P}_1, \overline{P}_2 \rangle = \langle \overline{P}_1, \overline{P}_2 \tan\theta \rangle = \overline{P}_1 \langle 1, \tan\theta \rangle = \mu \overline{P}_{10} \langle 1, \tan\theta \rangle$$

where μ is a weight factor of generalized proportional loadings, $\overline{P}_{10}$ is the base load of $\overline{P}_1$. If the generalized limit load multiplier is denoted by ν, the generalized plastic limit solution is:

$$\langle \overline{P}_1, \overline{P}_2 \rangle_L = \nu \langle \overline{P}_1, \overline{P}_2 \rangle_0 = \nu \overline{P}_{10} \langle 1, \tan\theta \rangle, \tag{2.1}$$

where ν can be computed by a direct iterative algorithm as shown in the next section.

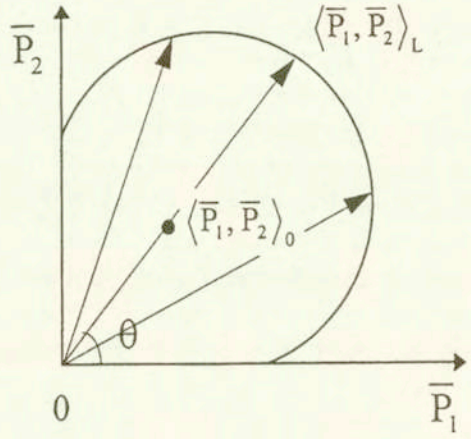

FIG. 1. Radial loading path under two loading systems.

3. Iterative algorithm

Consider a 3-D rigid-perfectly plastic body V with the boundary S. The individually varying multi-loading system $\sum_m \overline{\mathbf{P}}_m$ (m is the number of loadings) is applied on S_σ, and the displacement constraint $u_i = 0$ is imposed on S_u. The plastic incompressibility condition $u_{i,i} = 0$ is satisfied in the body V. On the basis of the kinematic theorem of limit analysis and the finite element discretization technique, we have

$$\left(\sum\nolimits_m \mathbf{P}_m\right)^T \mathbf{U} \le \sum_{e=1}^{N} \int_{V_e} W_P dV \tag{3.1}$$

where W_P is the rate of plastic energy dissipation, $\mathbf{P}_m$ is the m-th equivalent nodal load vector corresponding to $\overline{\mathbf{P}}_m$, $\mathbf{U}$ is the nodal velocity vector, and N is the number of elements.

Adopting the von Mises yield criterion and Gauss integration method, one has

$$V\left(\sum\nolimits_m \mathbf{P}_{mo}\right)^T \mathbf{U} \le \sqrt{\frac{2}{3}}\sigma_y \sum\nolimits_{i\in \mathbf{I}} \rho_i \sqrt{\mathbf{U}^T \mathbf{K}_i \mathbf{U}} |\mathbf{J}|_i \tag{3.2}$$

where I is the set of all Gauss integration points, ρ_i is the integration weight, $|\mathbf{J}|_i$ is the Jacobian determinant $|\mathbf{J}|$ at the Gauss integration point i, ν is the general-

ized limit load multiplier, $\mathbf{P}_{mo}$ is the equivalent nodal load vector corresponding to the m-th base load of $\overline{\mathbf{P}}_{mo}$, $\mathbf{K}_i$ is the stiffness matrix at the Gauss point i, and σ_y is the yield stress of material.

The above inequality leads to the following discretized mathematical programming formulation:

$$\begin{cases} \nu = \min_{\mathbf{U}} : \sqrt{\dfrac{2}{3}}\sigma_y \sum_{i\in I} \rho_i \sqrt{\mathbf{U}^T \mathbf{K}_i \mathbf{U}} |\mathbf{J}|_i, \\ \text{s.t.} \left(\sum_m \mathbf{P}_{mp}\right) \mathbf{U} = \mathbf{1}, \\ \mathbf{U}^T (\mathbf{K}_V)_i \, \mathbf{U} = \mathbf{0} \ \forall i \in \mathbf{I}, \end{cases} \tag{3.3}$$

where the abbreviation "s.t." means "subject to", and the volumetric stiffness matrix $\mathbf{K}_V^e$ for each element can be expressed as

$$\mathbf{K}_V^e = (\mathbf{B}_V^e)^T \mathbf{B}_V^e, \tag{3.4}$$

in which the volumetric strain matrix is $\mathbf{B}_V^e = \operatorname{div} \mathbf{N}^e$ and $\mathbf{N}^e$ is the shape function matrix for each element. For convenience, the constant factor $\sqrt{\dfrac{2}{3}}\sigma_y$ is omitted temporarily in the following discussion.

Obviously, Eq. (3.2) is a non-linear mathematical programming problem, thus it is difficult to find an efficient search direction and the property of upper bound can not be guaranteed. Furthermore, the objective function of Eq. (3.3) is non-smooth. It is difficult to treat the rigid portion because of the singularity of the derivative of objective function over rigid zones. To overcome those difficulties, we perform a series of iterations to solve Eq. (3.3). At each iteration, the rigid and plastic zones are distinguished and the objective function and constraint conditions are suitably modified. Namely, before proceeding with the $(j+1)$-th iteration, we examine the strain value of every integration point and divide the set I of all integration points into the rigid zone subset R_{j+1} and the plastic zone subset P_{j+1}, i.e.:

$$\begin{aligned} I &= R_{j+1} \cup P_{j+1}, \\ R_{j+1} &= \{i \in I, \, \mathbf{U}_j^T \mathbf{K}_i \mathbf{U}_j = 0\}, \\ P_{j+1} &= \{i \in I, \, \mathbf{U}_j^T \mathbf{K}_i \mathbf{U}_j \neq 0\}. \end{aligned} \tag{3.5}$$

The determination of set R_{j+1} and P_{j+1} is essential for removing those points at the rigid state from the sum of integration points of the objective function, so as to ensure that the next iteration can proceed normally. Meanwhile, we can also physically find the distribution of the plastic and rigid zones during the iterative

process by Eq. (3.5). The following iterative formulation is then constructed to solve Eq. (3.3) directly:

$$
\begin{aligned}
&\nu = \min_{U} : \sum\nolimits_{i\in P_j} \frac{\rho_i |\mathbf{J}|_i \mathbf{U}^T \mathbf{K}_i \mathbf{U}}{\sqrt{\mathbf{U}_j^T \mathbf{K}_i \mathbf{U}_j}}, \\
&\text{s.t.} \ \left(\sum\nolimits_m \mathbf{P}_{m0}\right)^T \mathbf{U} = 1, \\
&\mathbf{U}^T (\mathbf{K}_V)_i \mathbf{U} = 0 \qquad \forall i \in P_j, \\
&\mathbf{U}^T \mathbf{K}_i \mathbf{U} = 0 \qquad \forall i \in R_j,
\end{aligned} \tag{3.6}
$$

where $\mathbf{U}_j$ is the nodal velocity array at the j-th iteration.

In the formulation (3.6), the additional constraint condition $(3.6)_4$ imposed on the rigid zone and the incompressibility condition $(3.6)_3$ imposed on the plastic zone can be introduced by the penalty function method. The normalization constraint $(3.6)_2$ can be enforced by the Lagrangian multiplier method. By applying the optimality conditions of the augmented objective function, the problem (3.6) is equivalent to solving the following linear algebraic equations:

$$
\begin{cases}
\sum_{i\in I} \rho_i |\mathbf{J}|_i \tilde{\mathbf{K}}_i \mathbf{U} = \lambda \sum_m \mathbf{P}_{m0}, \\
\left(\sum_m \mathbf{P}_{m0}\right)^T \mathbf{U} = 1,
\end{cases} \tag{3.7}
$$

where λ is the Lagrangian multiplier, and

$$
\tilde{\mathbf{K}}_i = \begin{cases}
\dfrac{\mathbf{K}_i}{\sqrt{\mathbf{U}_j^T \mathbf{K}_i \mathbf{U}_j}} + A_1 (\mathbf{K}_V)_i & \forall i \in P_j, \\
A_2 \mathbf{K}_i & \forall i \in R_j,
\end{cases} \tag{3.8}
$$

in which A_1 and A_2 are the penalty factors. In practice, the typical values of A_1 and A_2 vary from 10^6 to 10^{12}. Solving Eq. (3.7), we get the nodal velocity array $\mathbf{U}_j$ at step j, and then compute the generalized limit load multiplier ν_j by using Eq. $(3.3)_1$.

The iteration is initiated as follows:

$$
\begin{aligned}
&\min_{U} : \sum\nolimits_{i\in I} \rho_i |\mathbf{J}|_i \mathbf{U}^T \mathbf{K}_i \mathbf{U}, \\
&\text{s. t.} \ \left(\sum\nolimits_m \mathbf{P}_{m0}\right)^T \mathbf{U} = 1, \\
&\mathbf{U}^T (\mathbf{K}_V)_i \mathbf{U} = 0 \qquad \forall \mathbf{i} \in \mathbf{I}.
\end{aligned} \tag{3.9}
$$

From Eq. (3.9), we can obtain the initial values of $\mathbf{U}_0$ and ν_0.

The above iterative process is terminated when the following convergence criteria are satisfied:

$$\frac{|\nu_{j+1} - \nu_j|}{\nu_j} \leq \text{VOL1},$$

(3.10)

$$\frac{\|\mathbf{U}_{j+1}\mathbf{U}_j\|}{\|\mathbf{U}_j\|} \leq \text{VOL2},$$

where VOL1 and VOL2 are the desired accuracies of the calculation.

The authors of this paper have shown that the above iterative process leads to the limit load multiplier ν and to a collapse mechanism $\mathbf{U}$ through a convergent sequence with monotonically decreasing ν_j.

4. Applications

4.1. Cylindrical shell joined-both ends to rigid plates subjected to radial pressure and independent axial load

The geometry of a cylindrical shell joined at both ends to rigid plates, subjected to radial pressure and independent axial load and the arrangement of finite element mesh, are shown in Fig. 2.

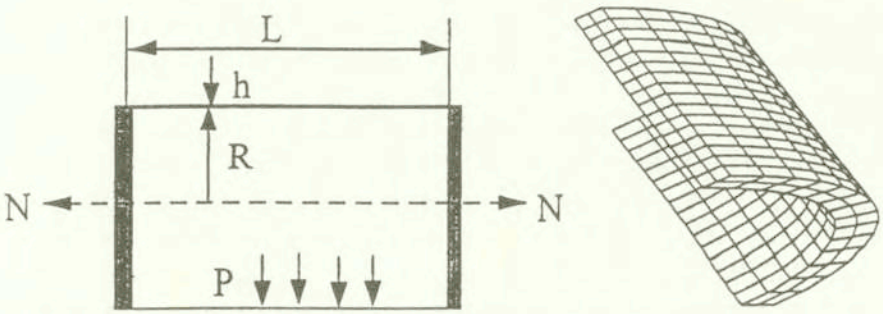

FIG. 2. Cylindrical shell joined at both ends to rigid plates, subjected to a radial pressure and an independent axial load, together with the finite element mesh used in this study.

Let $\omega^2 = \dfrac{L^2}{2hR}$, $p = \dfrac{PR}{\sigma_y h}$, $n = \dfrac{N}{2\pi R\sigma_y h}$, where σ_y is the uniaxial yield stress. HODGE and PANARELLI [11] solved this problem and presented both the lower and upper bound approximations of limit load for a von Mises material. ZHANG [10] also presented the solutions of this problem using the limit analysis and

considering initial constant loadings and proportional loadings. The results of our solution fall between the lower bound and upper bound given by HODGE and PANARELLLI [11], and are in a good agreement with the solutions of Zhang, as shown in Fig. 3. Obviously, this indicates that the proposed radial loading path scheme is reasonable and feasible and the above numerical procedure is effective.

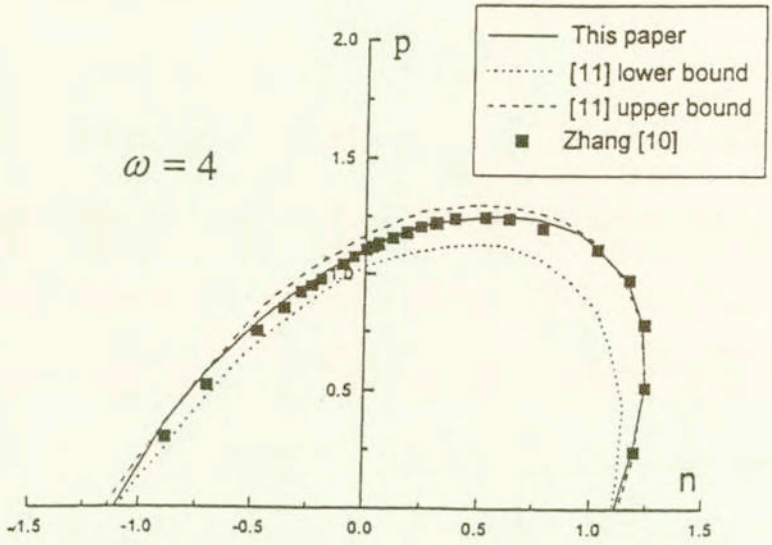

FIG. 3. The limit load interaction curves obtained by different methods.

4.2. Plastic collapse analysis of defective pipelines under internal pressure, axial tension and bending moment

4.2.1. Determination of plastic limit load. The geometry of defective pipeline subjected to internal pressure (P), axial tension (N) and bending moment (M) is shown in Fig. 4. The defects considered here are part-through slots of various geometrical configurations. The engineering situation considered here has a practical important background in the pipeline industry. Here the axial tension (N) includes the independent axial tension N_1 and the additional axial tension N_2 induced by an internal pressure P, i.e. $N_2 = P\pi R_i^2$, where R_i is the inner radius of a pipe. Using the proposed numerical algorithm,we perform the plastic collapse analysis of a cylindrical pipe with different shapes and sizes of part-through slots under internal pressure,bending moment and axial force(more than 1.000 examples have been computed here). The material is assumed to be rigid-perfectly plastic. The radius ratio kk (i.e. the ratio of the external to internal radius) of the pipe is 1.20. The pipe thickness is $T = 20$ mm. The yield stress σ_y of the material is 245 MPa.

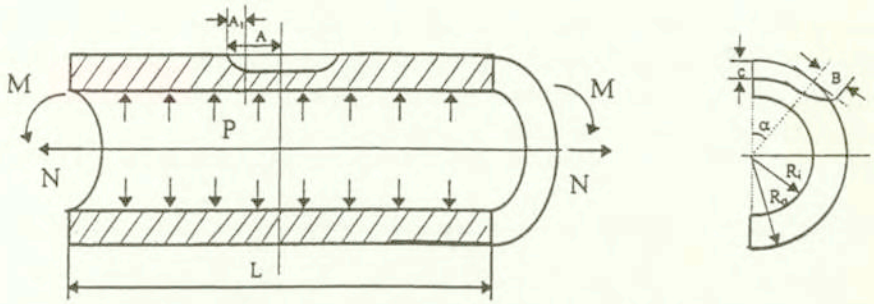

FIG. 4. Geometry of the pipeline with a part-through slot subjected to internal pressure, axial tension and bending moment.

Considering the symmetry of structure, we take a quadrant of the pipeline with four kinds of slots and discretize it by 3-D 20-node isoparametric finite elements. For various sizes of pipes and part-through slots, the finite element analysis meshes are defined by using 500–1000 elements and 600–1500 nodes. The corresponding displacement constraints are imposed on the symmetric boundaries. In order to optimize the numerical efficiency and accuracy, the finite element mesh should be chosen appropriately for a cylinder with a slot so as to make the distribution of the elements around the slot as even and neat as possible, and more dense than those located in other parts of the cylinder.

We define the following non-dimensional parameters:

$$
\begin{aligned}
m &= M/M_0, \quad M_0 = 4R^2T\sigma_y, \\
p &= \frac{P}{P_0}, \quad P_0 = \frac{2}{\sqrt{3}}\sigma_y \quad \ln\frac{R_0}{R_i}, \\
n &= N/N_0, \quad N_0 = \pi(R_0^2 - R_i^2)\sigma_y,
\end{aligned}
\tag{4.1}
$$

with the mean radius of a pipe $R = \dfrac{R_i + R_0}{2}$ and the wall-thickness $T = R_0 - R_i$.

The rectangular slot is analzed first because this kind of slot is relatively dangerous. For the pipeline with a rectangular slot under an internal pressure, we compute the limit loads of pipes for the combinations of the depth of slot $C/T = 0,\ 0.1,\ 0.2,\ 0.3,\ 0.4,\ 0.5,\ 0.6,\ 0.7,\ 0.8,\ 0.9$, the width of slot $\alpha/\pi = 0,\ 0.02,\ 0.04,\ 0.07,\ 0.1,\ 0.2,\ 0.3,\ 0.4,\ 0.5,\ 0.6,\ 0.7,\ 0.8,\ 0.9$ and the length of slot $A/\sqrt{RT} = 0,\ 0.2,\ 0.4,\ 0.6,\ 0.8,\ 1.0$. The calculated results are shown in Fig. 5. We can see that the width of the slot has some effect on the limit loads of pipes. When the depth of the slot is relatively small (e.g. $C/T < 0.2$), variation of the width of the slot has a small effect on the limit loads of pipes; when the depth of the slot is relatively large (e.g. $C/T > 0.5$), the variation of the width of

the slot affects the limit loads of pipes remarkably. With the depth of the slot increasing, the effects of the width of the slot on the limit loads of pipes are more pronounced. We can also see from Fig. 5 that when the width of the slot exceeds a critical value (e.g. $\alpha/\pi > 0.65$) for relatively large axial length of the slot, variation of the width of the slot has a small effect on the limit loads of pipes.

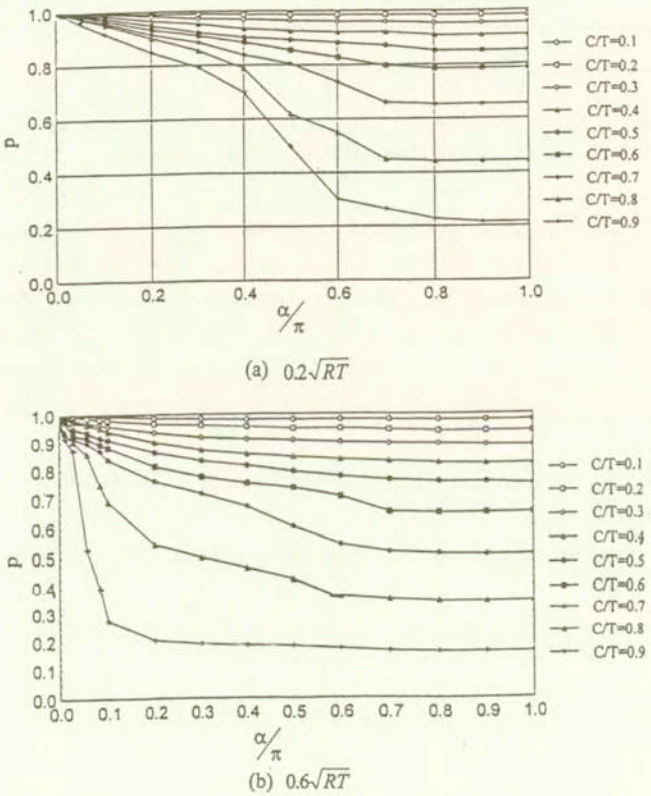

(a) $0.2\sqrt{RT}$

(b) $0.6\sqrt{RT}$

FIG. 5. Effects of the width of a slot on the limit moments of pipeline under a bending moment.

For the pipeline with a rectangular slot under a bending moment, we compute the limit loads of the pipe for the combinations of the circumferential length of the slot $\alpha/\pi = 0.1, 0.2, 0.3, 0.4, 0.5, 0.6, 0.7, 0.8, 0.9, 1.0$, the depth of the slot $C/T = 0.1, 0.2, 0.3, 0.4, 0.5, 0.6, 0.7, 0.8, 0.9$ and the length of the slot $A/\sqrt{RT} = 0, 0.2, 0.5, 0.8, 1.0, 2.0, 3.0, 4.0, 5.0, 6.0, 7.0$. The calculated results are shown in Fig. 6. We can see that when the axial length of the slot exceeds a critical value (e.g. $A/\sqrt{RT} = 1.46$), the variation of the axial length of the slot has no effect on the limit moment of pipes.

The plastic collapse loads of pipelines with four different shapes and sizes of part-through slots under the combined action of an internal pressure, axial

tension and bending moment are computed and analyzed here. The limit load interaction curves of pipeline under the combined actions of internal pressure and bending moment, bending moment and independent axial tension, and internal pressure and independent axial tension, are respectively plotted in Figs. 7 – 9. From these three figures, we can obviously see that the small area slot has a little effect on the limit load curves of the pipelines. The axial slot affects greatly the limit loads of pipelines under an internal pressure, and affects sllghtls the loads under the combined action of bending moment and axial force. On the contrary, for the circumferential slot, the limit loads of pipelines are affected more under the combined action of bending moment and axial force than under the internal pressure. For a large area slot, the corresponding failure mode is not a global collapse but a local collapse, and hence the limit loads of pipelines decrease considerably.

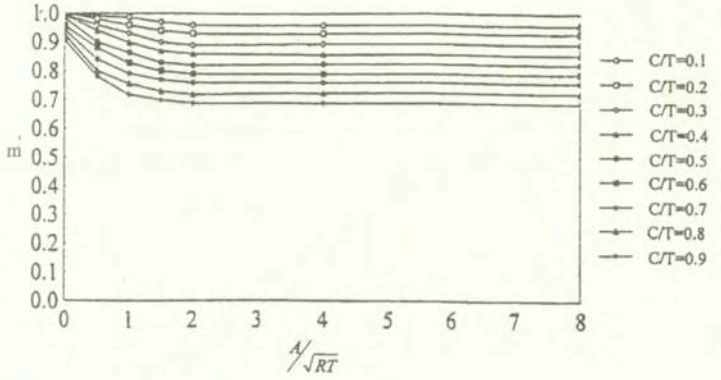

(a) $\alpha/\pi = 0.3$

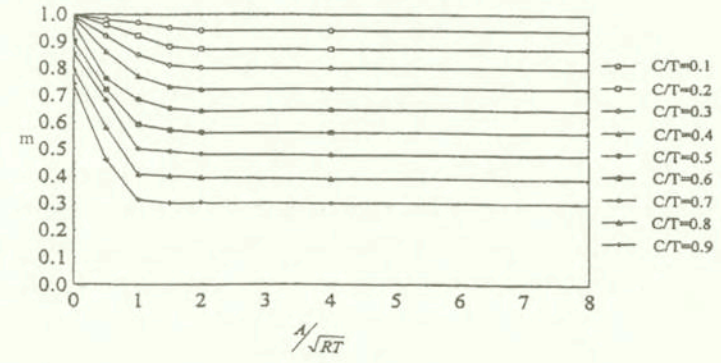

(b) $\alpha/\pi = 0.6$

FIG. 6. Effects of the axial length of a slot on the limit moments of popeline under a bending moment.

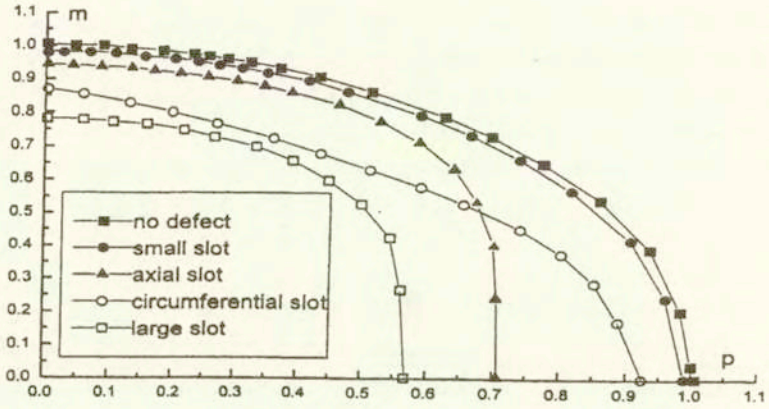

FIG. 7. The limit load interaction curves of pipeline under internal pressure and bending moment.

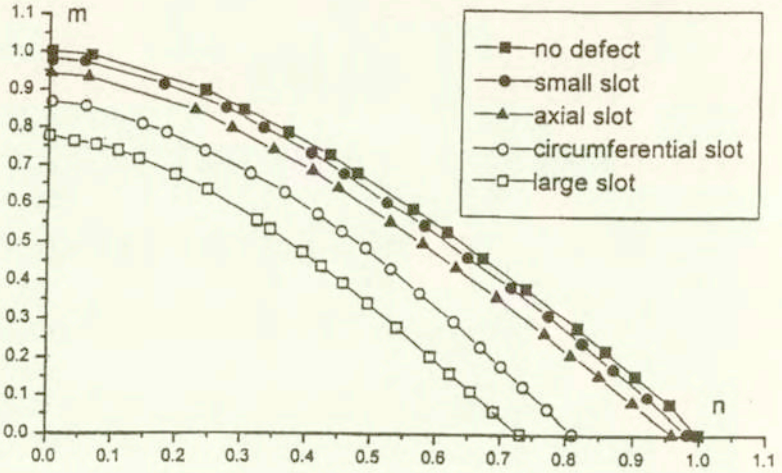

FIG. 8. The limit load interaction curves of a pipeline under axial tension and bending moment.

Some conclusions can also be drawn here. The effects of ellipsoidal and axially rectangular part-through slots on the limit loads of pipelines, which are induced by an internal pressure, are much greater than those induced by a bending moment. Therefore, the pipeline with the above two defects is relatively safe under a bending moment. But under the action of an internal pressure, the load-carrying capacity of a pipeline decreases considerably due to the axial rectangular slot. For the pipeline under the action of a bending moment or an axial force, an axial slot is safer than a circumferential slot. For the pipeline under an internal pressure, an axial slot is more dangerous. Furthermore, on the basis of these solutions of limit load interaction curves, the integrity assessment of pipeline with

various kinds of slots can be performed by the widely used integrity assessment procedures such as Nuclear Electric's (the former CEGB in the UK) R5 and R6 (the standards and codes of assessment of defective structures).

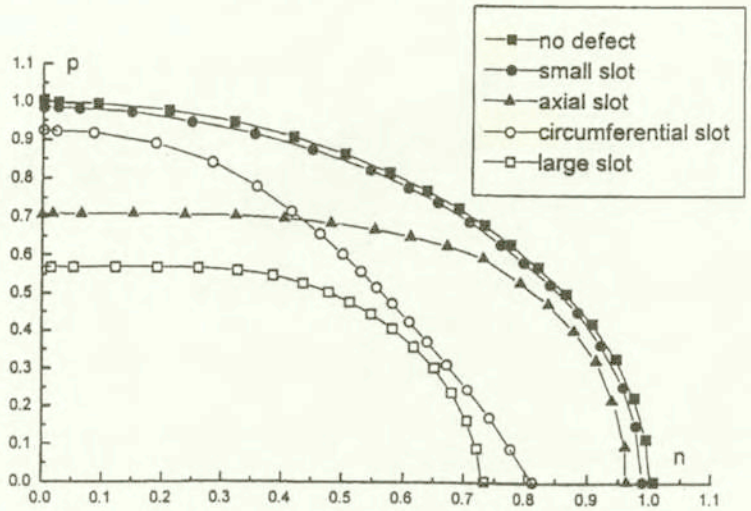

FIG. 9. The limit load interaction curves of a pipeline under internal pressure and independent axial tension.

4.2.2. The failure modes. For the pipeline with a small area slot, when the internal pressure reaches the limit load, most regions of pipe are found to yield except some regions near the outside surface, which are still in rigid states, where the shaded area represents the plastic region. Large areas of plastic deformation develop in the pipe. When the pipeline reaches the limit state under a bending moment, most of the pipe starts to yield except the middle regions. When the limit state is reached under an axial force, almost the entire pipe becomes a plastic region. This failure mode is a global collapse, which is similar to that of a pipe without defects. Therefore, a small area slot has a small effect on the limit loads of a pipe under the above loading systems. For the pipeline with an axial slot, we can see from Fig. 10 that when the limit load is reached by an internal pressure, the part of pipe near the slot starts to yield and the other part of pipe is still rigid. In this case, with the rigid regions near the slot going into yielding, a local plastic hinge is formed around the slot. The ligament of the slot bulges towards the outside, and a local leakage may occur within the slot of the pipe. When the pipe with an axial slot reaches the limit state under the action of a bending moment, the corresponding failure mode is a global collapse and almost the same as that with a small slot. When the pipe with an axial slot reaches the limit state under an axial force, a large region near the slot goes into yielding and

extends in the direction of 45 degrees to the axial direction. These failure modes can also confirm the previously calculated results for the limit loads of the pipe with an axial slot, namely, the axial slot has a great effect on the limit load of pipe under an internal pressure and has a small effect under a bending moment and an axial force.

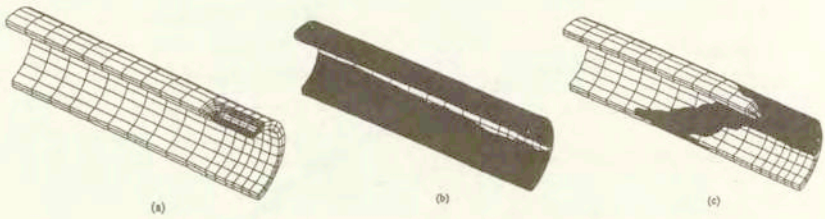

FIG. 10. Failure mode of a pipeline with an axial slot: a) under internal pressure; b) under bending moment; c) under axial tension.

For the pipeline with a circumferential slot, when the pipe reaches the limit state under an internal pressure, bending moment or axial force, the failure mode of the pipe is generally a local collapse. The local character of failure mode is more pronounced in the pipe under a bending moment and an axial force. This demonstrates that the circumferential slot has a greater effect on the limit load of the pipe under a bending moment or an axial force, and has a relatively small effect under an internal pressure.

For the pipeline with a large area slot, we can see from Fig. 11 that the failure mode is again a local collapse around the slot. This demonstrates that a large area slot has a greater effect on the limit loads of pipelines.

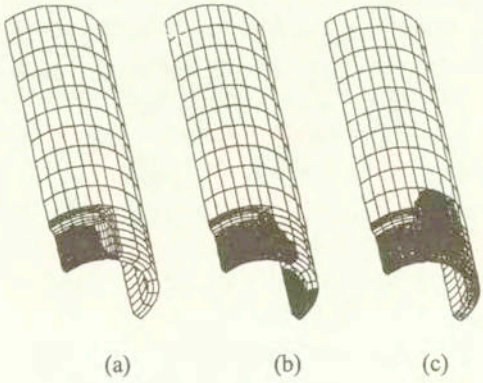

FIG. 11. Failure mode of a pipeline with a large area slot: a) under internal pressure; b) under bending moment; c) under axial tension.

5. Conclusions

By using an iterative algorithm for kinematic limit analysis of 3-D structures, a plastic collapse analysis of pipelines with part-through slots has been performed here under internal pressure, bending moment and axial force (more than 1.000 examples have been computed). The main conclusions can be drawn as follows:

1) The proposed iterative algorithm is efficient and reliable for performing the plastic collapse analysis of 3-D problems with complicated geometric forms and loading conditions.

2) The failure modes for defective pipelines include a global collapse and a local leakage. Corresponding to the former, the plastic load-carrying capacity of a pipeline is less affected. Corresponding to the latter, a plastic hinge is generally formed around the slot and the plastic load-carrying capacity of a pipeline decreases. Which failure mode occurs actually at the limit state for a defective pipeline should be determined by the size, position and orientation of the slot.

3) For the pipeline with a rectangular slot under an internal pressure, the width of slot has some effect on the limit load-carrying capacity of pipes, which is great, especially when the depth of slot is relatively large. The effects of the width of slot on the limit loads of pipes should not be neglected when the assessment of the remaining strength of pipes with slots is performed. For the pipeline with a rectangular slot under a bending moment, when the axial length of the slot exceeds a critical value (e.g. $1.46\sqrt{RT}$), the variation of the axial length of the slot has no effect on the limit moments of the pipes.

4) The small area slot has a small effect on the plastic load-carrying capacity of a pipeline, which collapses globally. For a pipeline with a large area slot, the corresponding load-carrying capacity decreases considerably due to a plastic hinge around the slot at the limit state. A local leakage generally occurs within the slot in this case. It is relatively dangerous to use such a pipeline. The axial slot has a great effect on the limit load of a pipeline under an internal pressure, and has a small effect under a bending moment and an axial force. The conclusion is opposite to the above for the circumferential slot.

Acknowledgements

The present study was supported by the Ministry of Science and Technology of China (96-918-02-03-02). This support is gratefully acknowledged.

References

1. R. SESHADRI and D. L. MARRIOTT, *On relating the reference stress, limit load and the ASME Stress Classification Concepts*, International Journal of Pressure Vessel & Piping, **56**, 387–408, 1993.

2. R. SESHADRI and C. P. D. FERNANDO, *Limit loads of mechanical components and structures using the GLOSS R-NODE method*, Journal of Pressure Vesssel Technology, **114**, 201–208, 1992.

3. D. MACKENZIE, C. NADARAJAH, J. SHI and J. T. BOYLE, *Simple bounds on limit loads by elastic finite element analysis*, Journal of Pressure Vesssel Technology, **115**, 27–31, 1993.

4. L. QIAN and Z. WANG, *Structural limit and shakedown analysis: A thermoparameter method*, Proc. ASME Pressure Vessel and Piping Conf., Nashnille, TN, **87**, 47–53, 1990.

5. T. BELYTSCHKO, *Plane stress shakedown analysis by finite elements*, International Journal of Mechanical Science, **14**, 619–625, 1972.

6. L. CORRADI and A. ZAVELANI, *A linear programming approach to shakedown analysis of structures*, Computer Methods in Applied Mechanics and Engineering, **3**, 37–53, 1974.

7. H. HUH and W. H. YANG, *A general algorithm for limit solutions of plane stress problems*, Int. J. Solids Structures, **28**, 6, 727–738, 1991.

8. Y. H. LIU, Z. Z. CEN and B. Y. XU, *A numerical method for plastic limit analysis of 3-D structures*, Int. J. Solids Structures, **32**, 1645–1658, 1995.

9. H. F. CHEN, Z. Z. CEN, B. Y. XU and S. G. ZHAN, *A numerical method for Reference stress in the evaluation of structure integrity*, International Journal of Pressure Vessel & Piping, **71**, 47–53, 1997.

10. Y. G. ZHANG, P. ZHANG and W. M. XUE, *Limit analysis considering initial constant loadings and proportional loadings*, Computational Mechanics, **14**, 229–234, 1994.

11. M. A. SAVE and C. E. MASSONNET, *Plastic analysis and design of plates, shells and disks*, North-Holland Publish Co., 1972.

Received January 10, 2000; revised version May 15, 2000.